Journal of the Serbian Chemical Society
JSCS-info@shd.org.rs • www.shd.org.rs/JSCS
J. Serb. Chem. Soc. 86 (2) S44–S57 (2021) *Supplementary material*

SUPPLEMENTARY MATERIAL TO

Synthesis, characterization, antimicrobial screening and cytotoxic properties of Cu(II) and Zn(II) complexes with a bidentate hydroxylated 1,3-diaryl-2-propene-1-one ligand

PRAVINKUMAR PATIL[1] and SAINATH ZANGADE[2]

[1]Research Laboratory, Department of Chemistry, N.E.S. Science College, Nanded-431605 (MS), India and [2]Department of Chemistry, Madhavrao Patil, ACS College, Palam, Dist. Parbhani-431720 (MS), India

J. Serb. Chem. Soc. 86 (2) (2021) 153–164

TABLE S-I. Preparation of complexes **C1**–**C10**

Metal chloride	Ligand*		Complex[a,b]	
Amount taken for synthesis, mg (0.25 mmol)	Molecular formula	Amount taken for synthesis, mg (0.50 mmol)	Molecular formula	Yield, %
43	$C_{19}H_{11}O_3I_3$	334	$CuC_{38}H_{20}O_6I_6$	58
43	$C_{19}H_{12}O_2BrCl$	194	$CuC_{38}H_{22}O_4Br_2Cl_2$	60
43	$C_{19}H_{12}O_2BrCl_2$	211	$CuC_{38}H_{20}O_4Br_2Cl_4$	62
43	$C_{19}H_{12}O_2BrCl_2$	211	$CuC_{38}H_{20}O_4Br_2Cl_4$	54
43	$C_{19}H_{13}O_4Br$	193	$CuC_{38}H_{24}O_8Br_2$	63
34	$C_{19}H_{15}O_2Br$	192	$ZnC_{40}H_{28}O_6Br_2$	61
34	$C_{19}H_{12}O_2Br_2$	216	$ZnC_{38}H_{22}O_4Br_4$	59
34	$C_{19}H_{13}O_3Br$	185	$ZnC_{38}H_{24}O_6Br_2$	57
34	$C_{19}H_{12}O_2BrF$	186	$ZnC_{38}H_{22}O_4Br_2F_2$	58
34	$C_{19}H_{13}O_4I$	216	$ZnC_{38}H_{24}O_8I_2$	62

* Physical data of ligand.[1]

CHARACTERIZATION

Bis((2-((E)-3-(2-hydroxy-3,5-diiodophenyl)acryloyl)-4-iodonaphthalen-1-yl)oxy)copper(II) (***C1***). Yield: 58 %; brown solid; m.p.: >300 °C decomposition; FTIR (KBr, cm^{-1}): 3434.8 (s, OH), 1643.2 (m, C=O), 1433.2 (m, C=C), 1207.2 (m, CO), 558.3 (m, CuO); ^{1}H-NMR (500 MHz, DMSO, δ / ppm): 5.41 (2H, *s*), 7.11 (2H, *d*, J = 16 Hz), 7.74 (2H, *d*, J = 16 Hz), 7.76-8.57 (14H, *m*); ^{13}C-NMR (125 MHz, DMSO, δ / ppm): 89.38, 100.22, 108.07, 113.10, 123.62, 136.50, 140.74, 147.81, 151.74, 164.62, 172.00, 183.31, 188.50; ESR: $g_{\|}$: 2.2497, $g_{\perp}$: 2.0972.

Bis((4-bromo-2-((E)-3-(4-chlorophenyl)acryloyl)naphthalen-1-yl)oxy)copper(II) (***C2***). Yield: 60 %; brown solid; m.p.: >300 °C decomposition; FTIR (KBr, cm^{-1}): 3410.6 (s, OH), 1523.5 (m, C=O), 1491.2 (m, C=C), 1256.5 (m, C-O), 526.5 (m, Cu-O); ^{1}H-NMR (500 MHz, DMSO, δ / ppm): 7.28 (2H, *d*, J = 16 Hz), 7.60 (2H, *d*, J = 16 Hz), 7.76-8.36 (18H, *m*); ^{13}C-

NMR (125 MHz, DMSO, δ / ppm): 92.83, 104.14, 109.80, 125.98, 134.46, 145.14, 148.91, 159.75, 174.20, 177.19.

Bis((4-bromo-2-((E)-3-(2,6-dichlorophenyl)acryloyl)naphthalen-1-yl)oxy)copper(II) ***(C3)***. Yield: 62 %; brown; m.p.: >300 °C decomposition; FTIR (KBr, cm^{-1}): 3463.7 (s, OH), 1635.1 (m, CO), 1606.2 (m, C=C), 1255.7 (m, C-O), 599.4 (m, Cu-O).

Bis((4-bromo-2-((E)-3-(2,4-dichlorophenyl)acryloyl)naphthalen-1-yl)oxy)copper(II) ***(C4)***. Yield: 54 %; brown; m.p.: >300 °C decomposition; FTIR (KBr, cm^{-1}): 3463.8 (s, OH), 1633.8 (m, C=O), 1572.7 (m, C=C), 1251.2 (m, C-O), 601.9 (m, Cu-O); ^{1}H-NMR (500 MHz, DMSO, δ / ppm): 7.10 (2H, *d*, *J* = 16 Hz), 7.53 (2H, *d*, *J* = 16 Hz), 7.67-8.72 (16H, *m*); ^{13}C-NMR (500 MHz, DMSO, δ / ppm): 82.94, 92.21, 106.19, 108.86, 128.18, 131.01, 151.58, 156.77, 160.54, 169.18, 171.69, 180.17, 182.69, 189.28.

Bis((4-bromo-2-((E)-3-(3,4-dihydroxyphenyl)acryloyl)naphthalen-1-yl)oxy)copper(II) ***(C5)***: Yield: 63 %; brown; m.p.: >300 °C decomposition; FTIR (KBr, cm^{-1}): 3416.3 (s, OH), 1611.8 (m, C=O), 1585.5 (m, C=C), 1253.5 (m, C-O), 594.1 (m, Cu-O).

Bis((4-bromo-2-((E)-3-(4-fluorophenyl)acryloyl)naphthalen-1-yl)oxy)zinc(II) ***(C9)***. Yield: 58 %; brown; m.p.: >300 °C decomposition; FTIR (KBr, cm^{-1}): 3434.6 (s, OH), 1635.1 (m, C=O), 1547.5 (m, C=C), 1249.8 (m, C-O), 468.7 (m, Cu-O); ^{1}H-NMR (500 MHz, DMSO, δ / ppm): 6.88 (2H, *d*, *J* = 16Hz), 7.47 (2H, *d*, *J* = 16 Hz), 7.76-8.58 (18H, m); ^{13}C-NMR (500 MHz, DMSO, δ / ppm): 101.32, 117.34, 125.19, 126.92, 131.95, 141.22, 142.63, 152.84, 156.45, 159.91, 165.09, 170.12, 183.16, 185.20,186.46; ESR: $g_{\parallel}$: 2.0509, $g_{\perp}$: 2.0066.

TABLE S-II. Crystal data and structure refinement

Complex	$[Cu(C_{19}H_{10}O_3I_3)_2]$	$[Cu(C_{19}H_{10}O_2BrCl_2)_2]$	$Zn(C_{19}H_{12}O_4I)_2$
Empirical formula	$Cu(C_{38}H_{20}O_6I_6)$	$Cu(C_{38}H_{20}O_4Br_2Cl_4)$	$ZnC_{38}H_{24}O_8I_2$
Formula weight	1397.53	905.73	927.78
Temperature, K	298	298	298
Crystal system	Orthorhombic	Orthorhombic	Orthorhombic
Space group	P b c a	P c a 21	P n m a
a / Å	16.8478	14.6387	22.2520
b / Å	12.4058	10.2508	17.6363
c / Å	27.8294	18.8246	11.3842
α / °	90	90	90
β / °	90	90	90
γ / °	90	90	90
Volume, $Å^3$	5816.64	2824.79	4467.65
Z	16	4	4
ρ_{calc} g / cm^{-3}	6.383	2.130	1.379
μ / cm^{-1}	5.744	38.815	30.222
Crystallite size, nm	24.70794	29.28896	13.16591
Dislocation density, nm^{-2}	1.63805	1.16571	5.76897
Micro strain	12.93231	7.72544	19.39073

MTT Assay

In-vitro anticancer activity was evaluated by MTT assay. The growth inhibitory activity of complexes was determined against liver cancer cells (HepG2). Activity data is presented in Fig. 26.

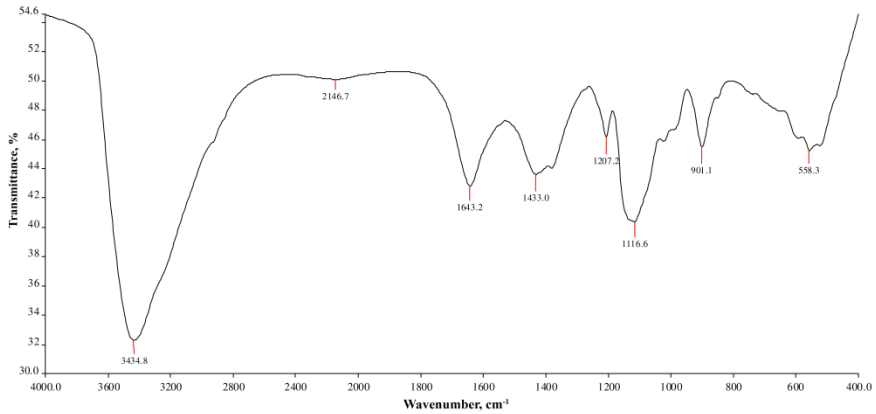

Figure S-1. FTIR Spectrum of complex C1

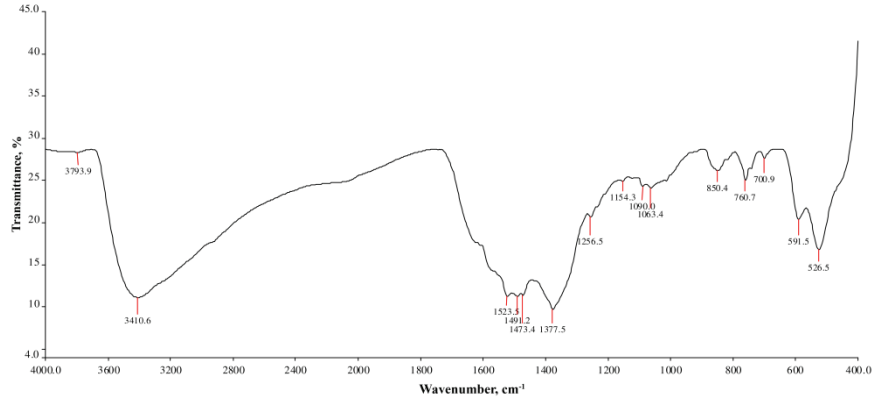

Figure S-2. FTIR Spectrum of complex C2

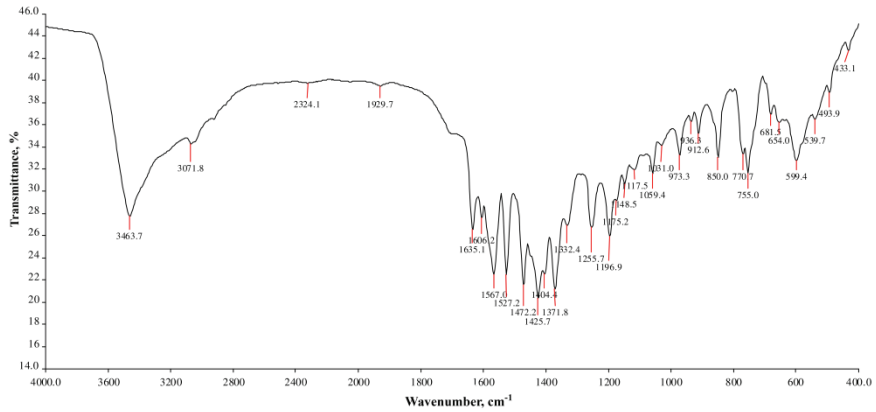

Figure S-3. FTIR Spectrum of complex C3

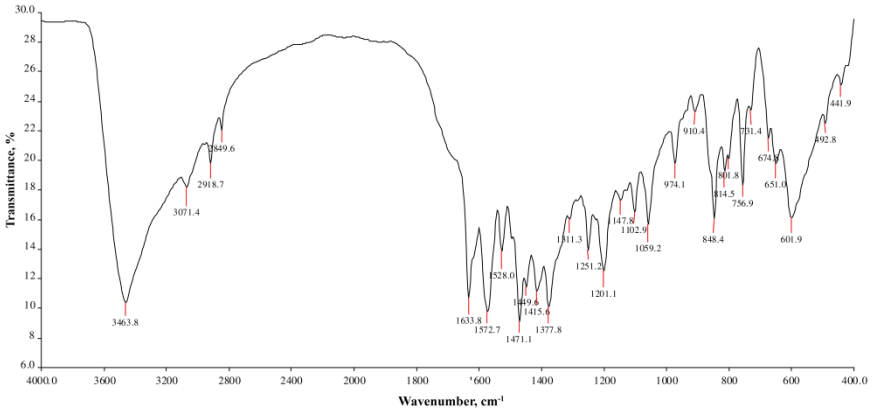

Figure S-4. FTIR Spectrum of complex C4

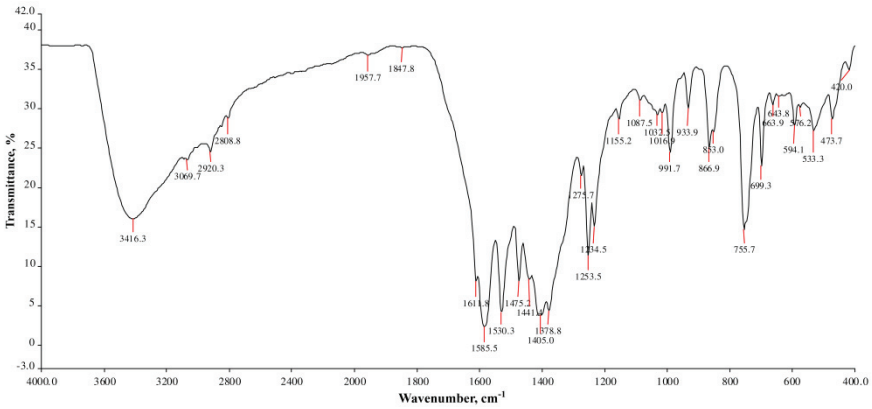

Figure S-5. FTIR Spectrum of complex C5

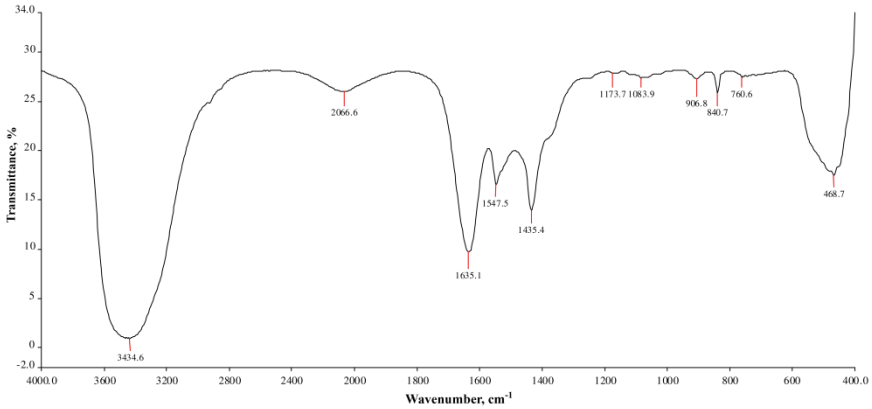

Figure S-6. FTIR Spectrum of complex C9

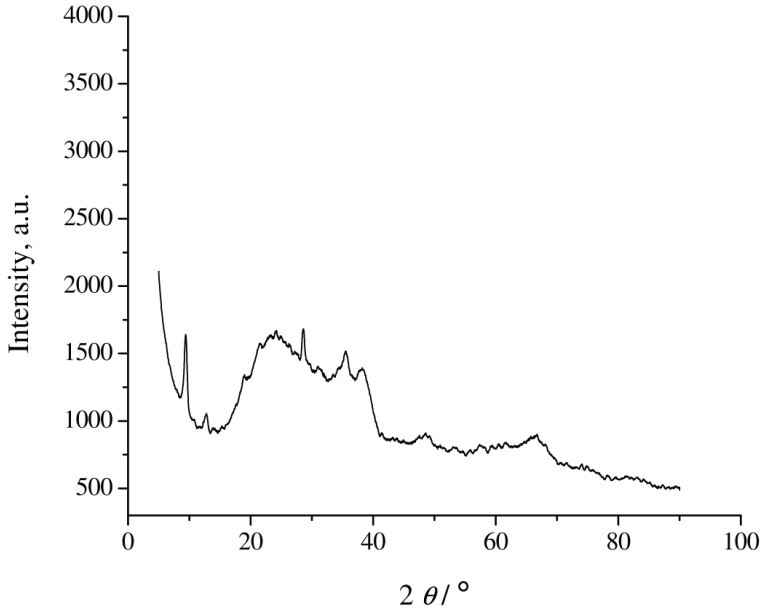

Figure S-7. XRD of complex C1

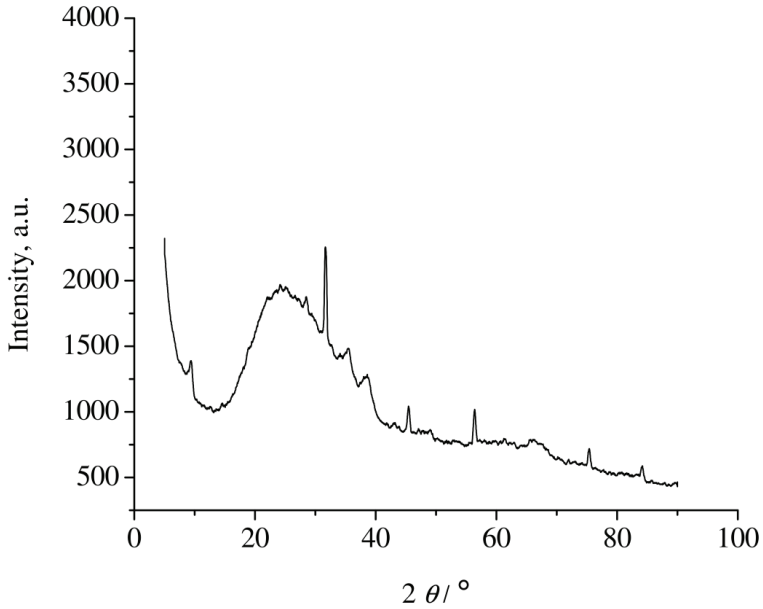

Figure S-8. XRD of complex C2

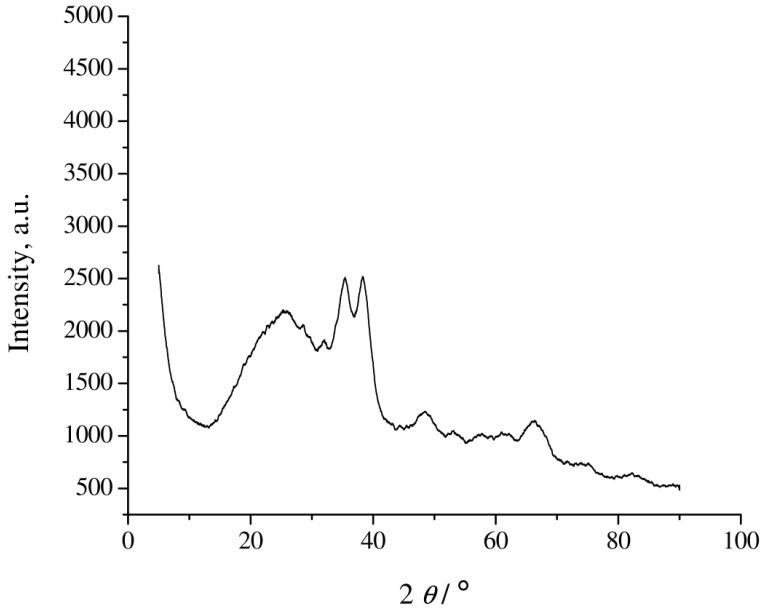

Figure S-9. XRD of complex C4

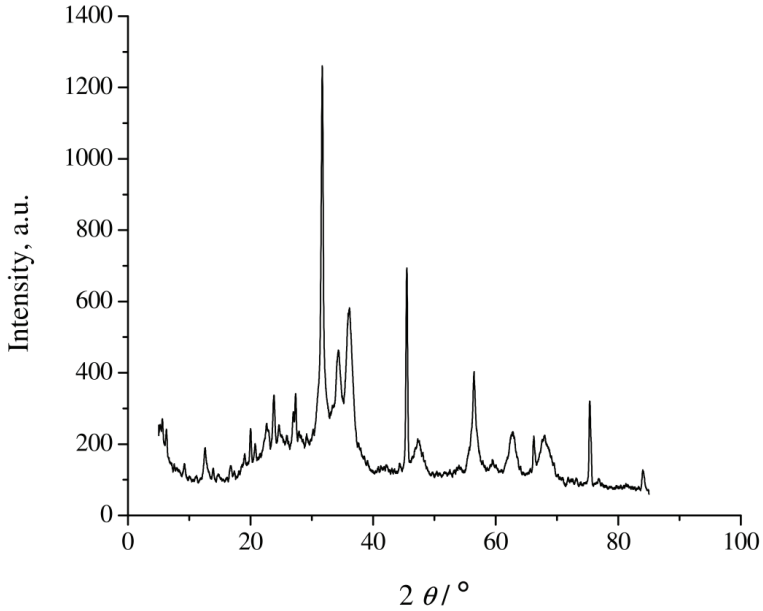

Figure S-10. XRD of complex C9

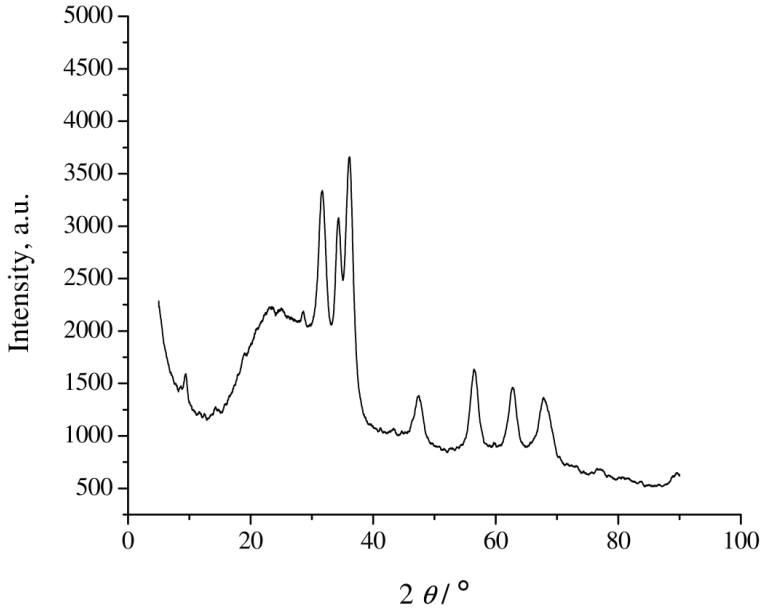

Figure S-11. XRD of complex C10

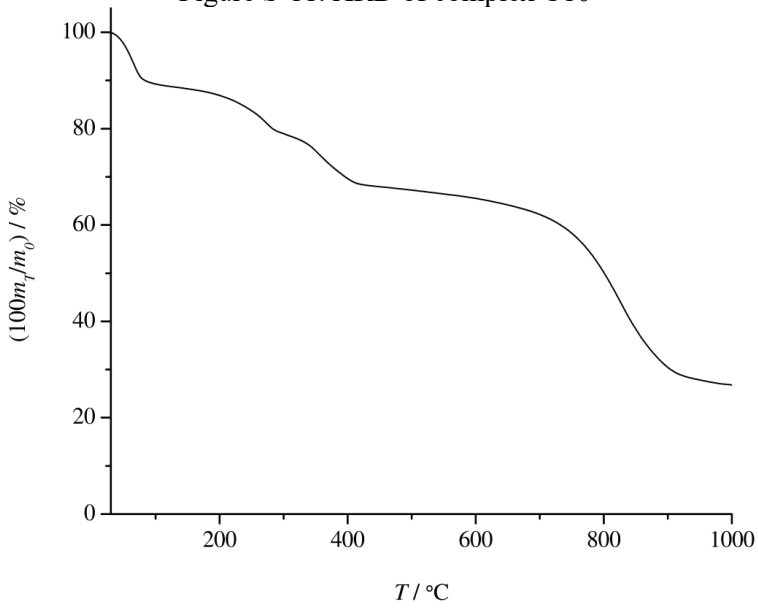

Figure S-12. TGA of complex C1

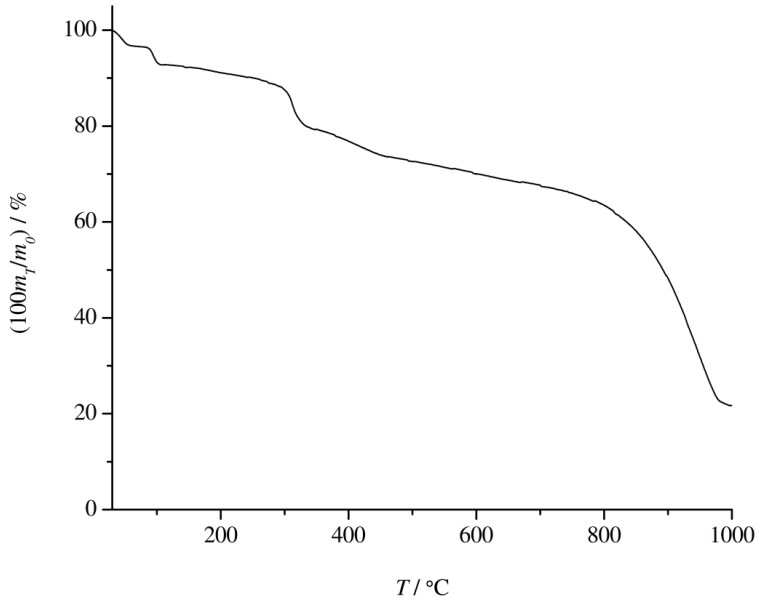

Figure S-13 TGA of complex C3

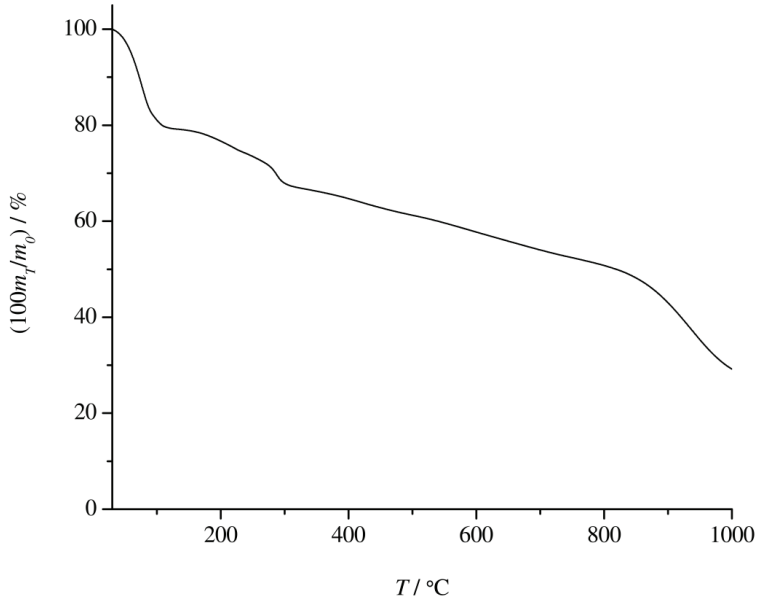

Figure S-14. TGA of complex C4

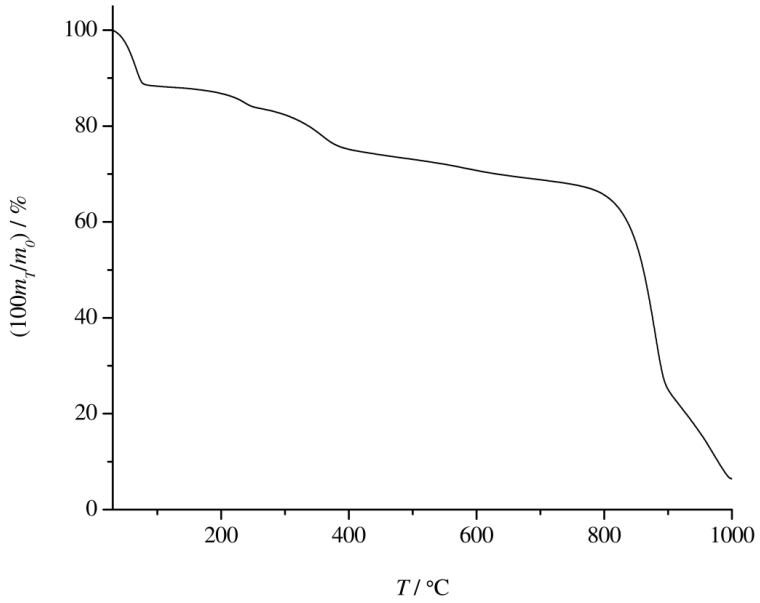

Figure S-15. TGA of complex C9

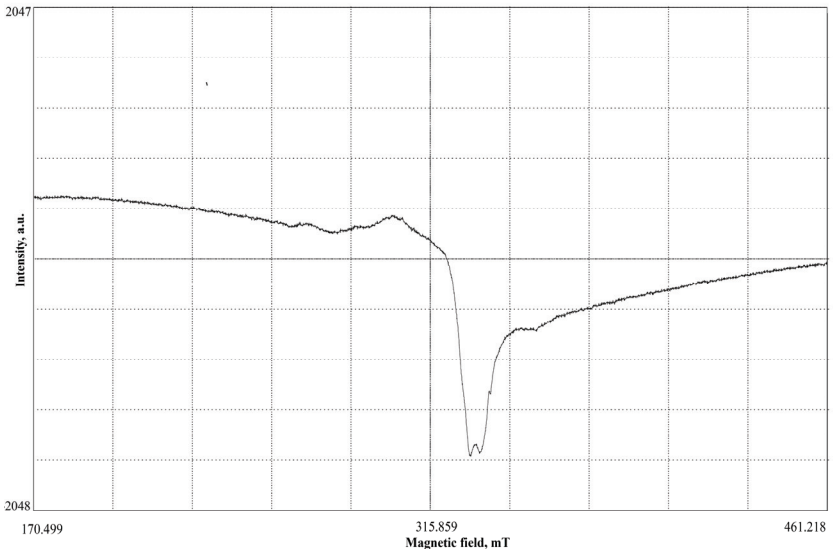

Figure S-16. ESR of complex C1

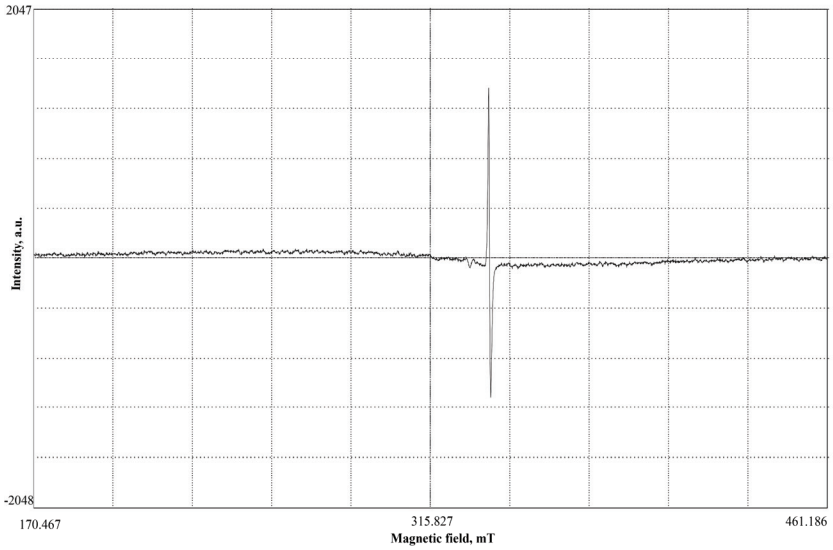

Figure S-17. ESR of complex C9

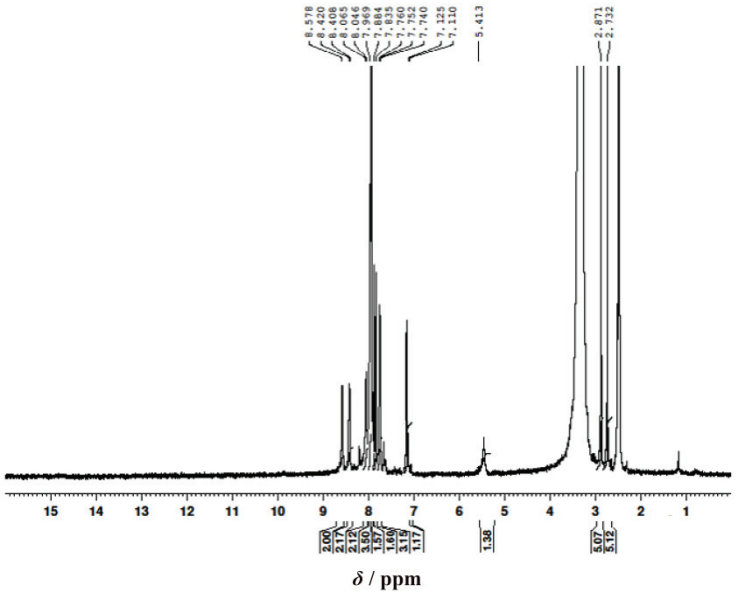

Figure S-18. ^{1}H NMR spectrum of complex C1

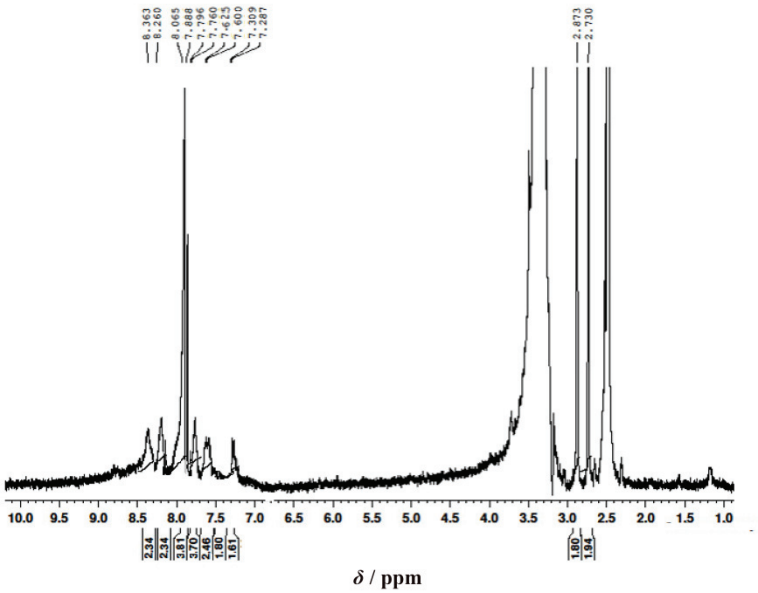

Figure S-19. ^{1}H NMR spectrum of complex C2

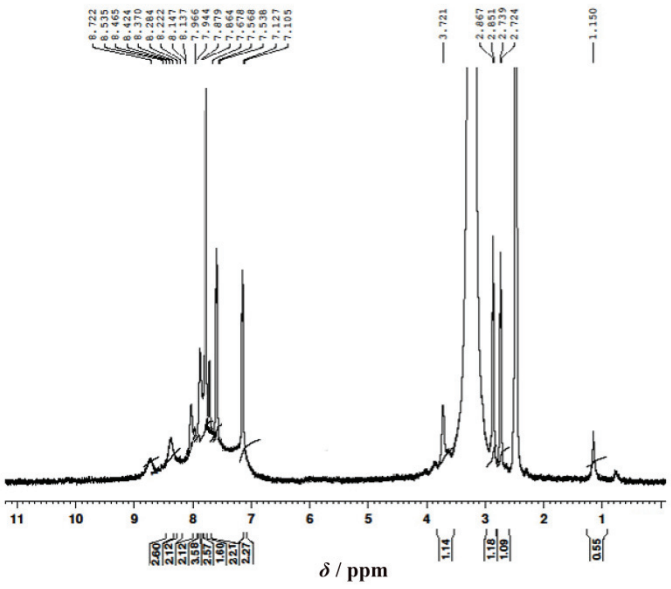

Figure S-20. ^{1}H NMR spectrum of complex C4

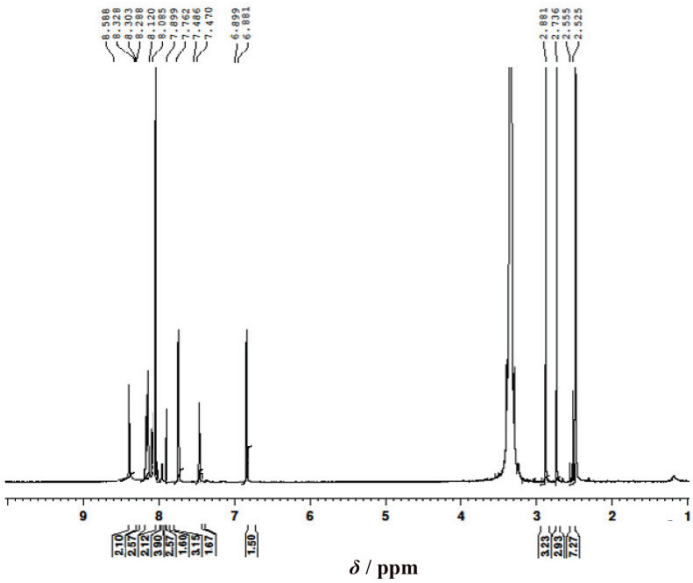

Figure S-21. ^{1}H NMR spectrum of complex C9

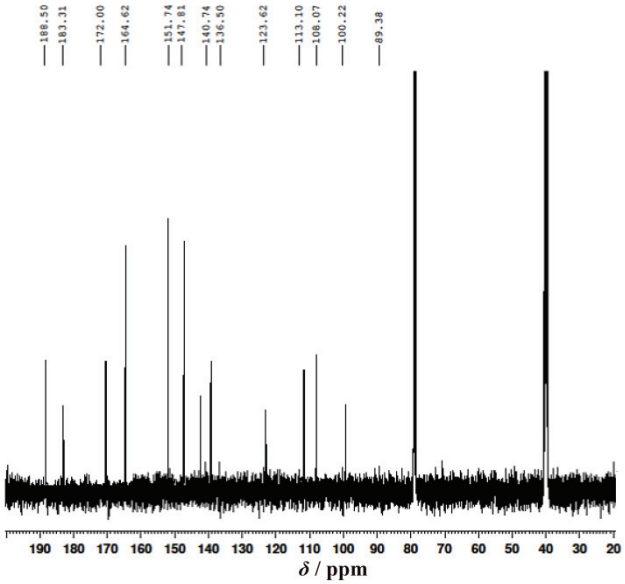

Figure S-22. ^{13}C NMR spectrum of complex C1

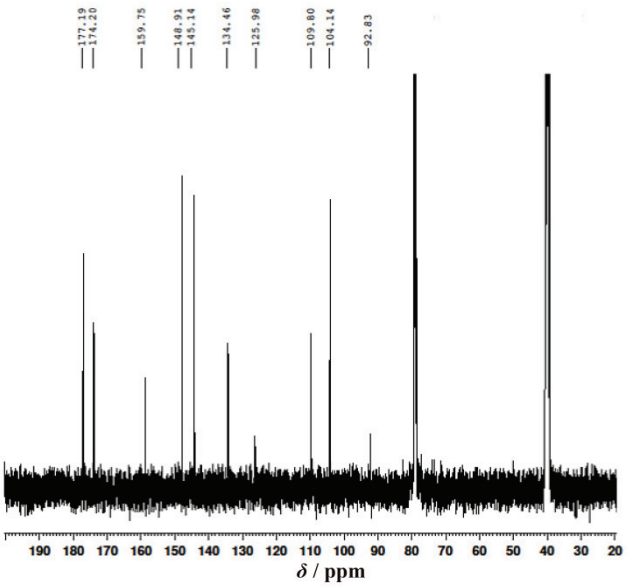

Figure S-23. ^{13}C NMR spectrum of complex C2

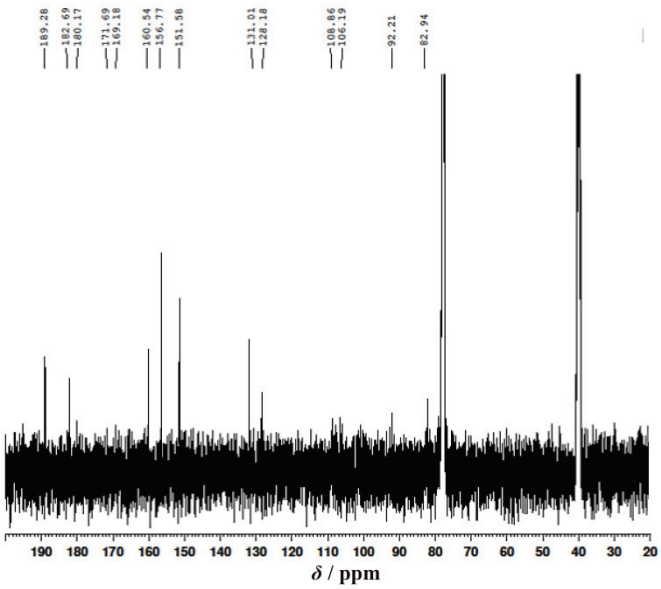

Figure S-24. ^{13}C NMR spectrum of complex C4

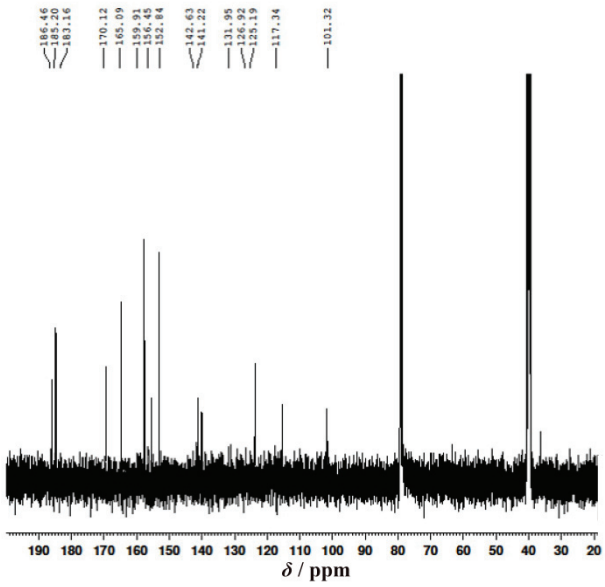

Figure S-25. ^{13}C NMR spectrum of complex C9

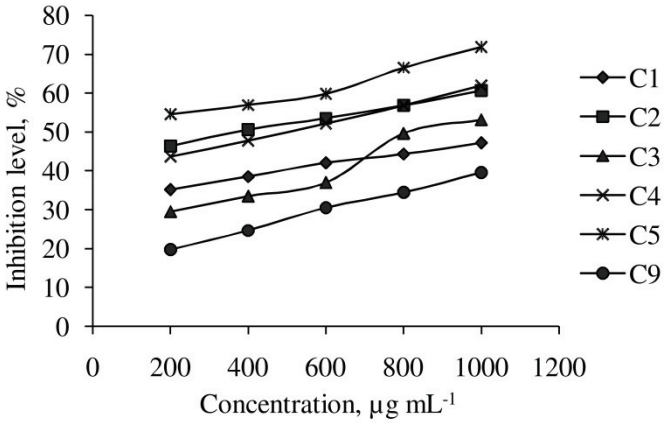

Figure S-26. Graph of sample concentration against the inhibition level

REFERENCE

1. P. Patil, P. A. Khan, S. Zangade, *Curr. Chem. Lett.* **9** (2020) 183–198 (http://www.growingscience.com/ccl/Vol9/ccl_2020_5.pdf)